High Pressure Polymorphism of β-TaON

K. Woodhead [a], S. Pascarelli [b], A. L. Hector [c], R. Briggs [d], N. Alderman [c] and P. F. McMillan[a] *

[a] Department of Chemistry, University College London, 20 Gordon Street, London WC1H 0AJ, UK.

[b] European Synchrotron Radiation Facility, BP 220, 38043, Grenoble Cedex, France.

[c] Chemistry, University of Southampton, Highfield, Southampton SO17 1BJ, UK.

[c] School of Physics and Astronomy, Centre for Science at Extreme Conditions, University of Edinburgh, Edinburgh EH9 3JZ, UK

The high pressure behavior of TaON was studied using a combination of Raman scattering, synchrotron X-ray diffraction, and X-ray absorption spectroscopy in diamond anvil cells to 70 GPa at ambient temperature. A Birch-Murnaghan equation of state fit for baddeleyite structured β-TaON indicates a high bulk modulus value K_o=328±4 GPa with K_o'=4.3. EXAFS analysis of the high pressure XAS data provides additional information on changes in the Ta-(O,N) and Ta-Ta distances. Changes in the X-ray diffraction patterns and Raman spectra indicate onset of a pressure induced phase transition near 33 GPa. Our analysis indicates that the new phase has an orthorhombic cotunnite-type structure but that the phase transition may not be complete even by 70 GPa. Similar sluggish transformation kinetics are observed for the isostructural ZrO_2 phase. Analysis of compressibility data for the new cotunnite-type TaON phase indicate a very high bulk modulus K_o ~ 370 GPa, close to the theoretically predicted value.

A Introduction

The semiconducting oxynitride compound TaON has received significant attention due to its interesting optical and electronic properties. Along with related tantalum nitrides (Ta_3N_5) it leads to an important class of low-toxicity yellow-red pigments.[1,2] More recently, TaON and Ta_3N_5 have been highlighted as potential photocatalysts in the water splitting reaction due to their band gaps that lie in the visible range, with the capacity to utilise a high proportion of the incident solar spectrum.[3-6]

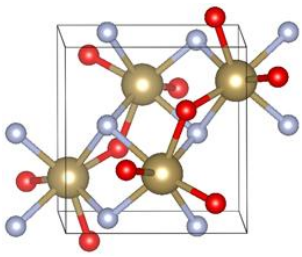

Figure 1. Sketch of the monoclinic ($P2_1/c$) unit cell of β-TaON highlighting the cation and anion coordination environments.[8] Oxygen atoms are shown in red, nitrogen atoms are blue, and the larger metal ions are shown as bronze (color online)

β-TaON was first reported by Brauer and Weidlein in 1965 as an intermediate phase occurring during the preparation of Ta_3N_5 by ammonolysis of Ta_2O_5, and they suggested that it was "probably of the baddeleyite (zirconium dioxide) type".[7] This monoclinic ($P2_1/c$) structure was later confirmed and

shown to contain ordered anions, with oxygen occupying 3-coordinate and nitrogen in 4-coordinate sites (Fig. 1).[8-10] Synthesis is typically achieved by ammonolysis of Ta_2O_5 under relatively fast flowing NH_3 at 850 °C,[6] though there is significant recent interest in alternative routes.[11] A lower flow rate results in γ-TaON, which is a metastable monoclinic polymorph (space group *C2/m*) with lower density than β-TaON.[12] An early report of a hexagonal α-TaON phase has since been discredited.[13] First principles calculations have been performed for both β- and γ-TaON polymorphs.[14,15] β-TaON has been shown to possess a valence band containing hybridised O 2p, N 2p and Ta 5d orbitals and has a direct band gap near 2.1 eV. Its bulk modulus was predicted to be K_o = 278 GPa, substantially higher than that for the isostructural refractory ceramic ZrO_2 (182 GPa).[16] Our results presented below indicate that K_o might have an even higher value than predicted.

Because β-TaON is isoelectronic with baddeleyite-structured ZrO_2 there is interest in the possibility of the oxynitride undergoing similar pressure-induced phase transitions. Zirconia is observed to begin to transform into an orthorhombic (*Pnma*) cotunnite structure above approximately 25 GPa at room temperature, although thermodynamic analysis indicates this phase should become stabilised above 7-8 GPa.[16] The high pressure cotunnite form of ZrO_2 has a very high bulk modulus value (K_o = 332 GPa) and has been proposed for use as a refractory high hardness material. Computational studies have indicated that a similar transformation should be present for β-TaON but initiated at higher pressure, above 30-31 GPa.[17,18] The calculated bulk modulus for this phase is very high (369 GPa) suggesting ceramic applications requiring high mechanical resistance. Additional polymorphs have also been predicted to occur at high pressure including a tetragonal bismoclite-type structure that might become stabilized above 38 GPa, and transition into cubic fluorite-type structures above P ~ 150 GPa.[17,18]

Reports of experimental high pressure studies of TaON are limited to one investigation, which found that the polycrystalline ceramic density and hardness properties were improved by sintering at 3-5.5 GPa and 920-1200 °C, but did not record any phase transformation behavior.[19] Here we report compression of TaON to 70 GPa at ambient temperature using a combination of synchrotron X-ray diffraction (XRD), Raman spectroscopy and energy dispersive X-ray absorption spectroscopy (XAS) with EXAFS analysis to monitor the compressibility and changes in the local Ta-(O,N) and Ta...Ta coordination environment. The data also provide the first evidence for a pressure-induced transformation into an orthorhombic cotunnite-structured polymorph with very high bulk modulus value above P=33 GPa as predicted theoretically.

B Experimental

β-TaON was prepared using a variation on previously published routes.[19,20] Amorphous Ta_2O_5 was obtained by dissolving $TaCl_5$ (5 g) in ethanol (100 cm^3), bubbling NH_3 gas through the mixture for 30 mins to form $Ta(OEt_2)_5$, then pouring into a dilute aqueous NH_3 (200 cm^3) to precipitate the amorphous oxide followed by filtering, washing and drying at 115 °C.[21] The precipitate was heated under flowing NH_3 at 900 °C for 16 hours to obtain phase pure β-TaON as a yellow powder as shown by powder X-ray diffraction (Siemens D5000; Cu-$K_{\alpha1}$ radiation) and combustion analysis (Medac Ltd: C <0.1%, H <0.1%, N 6.77%: theoretical: N 6.64%). The X-ray data were refined for the $P2_1/c$ structure using Rietveld techniques[22] to yield lattice parameters and atomic positions in excellent agreement with published values (Fig. 2, Table 1).[9] Previous authors bubbled NH_3 through water in order to obtain an appropriate partial pressure of H_2O for the formation of TaON rather than

Ta_3N_5.[20] We found that this approach led to crystallisation of Ta_2O_5 but no TaON formation. In our experiments, the gaseous NH_3 was passed through a Dreschel bottle containing a small quantity of water.

For high pressure experiments samples were loaded with NaCl or LiF as a pressure-transmitting medium into mechanically- or membrane-driven DACs with 300 μm culet diamonds and Re gaskets pre-indented to 25-30 μm, with 80-100 μm holes drilled by electro-erosion. Pressure was determined by fluorescence from ruby grains (~5 μm) placed within the sample chamber. Raman spectra were recorded using either home-built[23] or Renishaw InVia microbeam systems with 514.5 nm or 785 nm laser excitation. Angle dispersive XRD patterns were recorded at high pressure at beamline I15 of the Diamond Light Source (DLS) (β = 0.416746 Å) using a MAR345 image plate (exposure times 300 s). The data were integrated to provide conventional diffraction patterns using Fit2D[24] and Rietveld refinements were carried out using GSAS.[22]

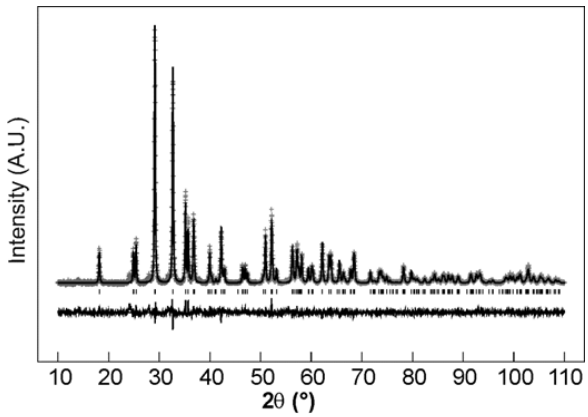

Figure 2. Rietveld fit to the XRD pattern of β-TaON (R_{wp} = 17.1%, R_p = 12.0%) synthesised in this study. Grey crosses mark the data points, the upper continuous line the fit, the lower continuous line the difference plot and tick marks indicate the allowed reflection positions for β-TaON in $P2_1/c$.

Table 1 Rietveld fitting parameters for β-TaON at ambient temperature and pressure.

	x	y	z	O*	U_{iso}/100 Å^2
Ta	0.2911(2)	0.0444(2)	0.2150(2)	1	1.51(4)
O	0.080(3)	0.331(2)	0.349(3)	1	1.2(3)
N	0.438(4)	0.751(3)	0.471(4)	1	1.2(3)

$P2_1/c$, a=4.9672(3), b=5.0351(3), c=5.1830(3) Å, β=99.627(2)°, R_{wp}=17.1%, R_p=12.0%. Published lattice parameters[9] a=4.968(1), b=5.037(1), c=5.185(1) Å, β=99.56(1)°. *O: fractional occupancy.

An ambient pressure XAS spectrum of β-TaON prepared by grinding the sample with powdered BN and pressing into an 8 mm disc was recorded at the Ta L_3 edge (9881 eV) at DLS beamline B18[25] using ionisation chamber detection. High-pressure XAS data were obtained up to 45 GPa using the energy-dispersive spectrometer at beamline ID24[26] of the European Synchrotron Radiation Facility (ESRF) with a 5×5 μm beam size and a FReLon Camera detector. XAS spectra were prepared for analysis using the Athena programme.[27] After background subtraction and normalisation, extended X-ray

absorption fine structure (EXAFS) data were fitted using the ARTEMIS programme[28,29] in conjunction with scattering models generated by FEFF. [30,31]

C Results and discussion

Raman spectroscopy

The ambient pressure Raman spectrum of β-TaON is shown in Figure 3. Eighteen Raman active modes are expected (9 A_g + 9 B_g): these can be identified as independent peaks or shoulders in the pattern between 100-1000 cm^{-1} and assignments made by comparison with density functional perturbation theory (DFPT) calculations [32,33] (Table 2).

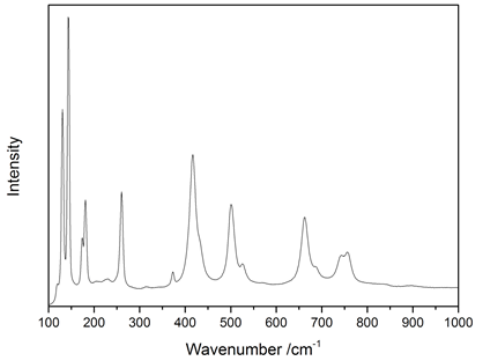

Figure 3. Raman spectrum of β-TaON at ambient conditions.

Table 2. Experimentally observed β-TaON Raman peaks compared with theoretically calculated values.[32,33]

Observed, cm^{-1}	Peak profile	Predicted, cm^{-1}	Symmetry
131	Strong, sharp	142	A_g
144	Strong, sharp	149	B_g
-	-	156	A_g
174	Sharp	187	B_g
181	Sharp	207	A_g
208	Weak, broad	-	-
228	Weak, broad	260	A_g
260	Sharp	266	B_g
315	Weak, broad	-	-
373	Sharp	387	B_g
417	Sharp	446	A_g
432	Shoulder	454	A_g
501	Sharp	531	B_g
526	Sharp	540	A_g
-	-	544	B_g
662	Sharp	694	A_g
686	Sharp	731	B_g
743	Sharp	779	B_g
756	Sharp	797	A_g
835	Weak, broad	872	B_g

High pressure Raman spectra of β-TaON were recorded up to 33 GPa in a first series of runs (Fig. 4). Changes in relative peak intensities were observed to begin at above approximately 13-16 GPa but no obvious features suggested the presence of a polymorphic phase transition. Later analysis of X-ray diffraction data to 58 GPa showed that a pressure-induced transformation into the high-density cotunnite phase does in fact occur with the transition process concentrated around 30-35 GPa range, although with premonitory effects possibly present at lower P.

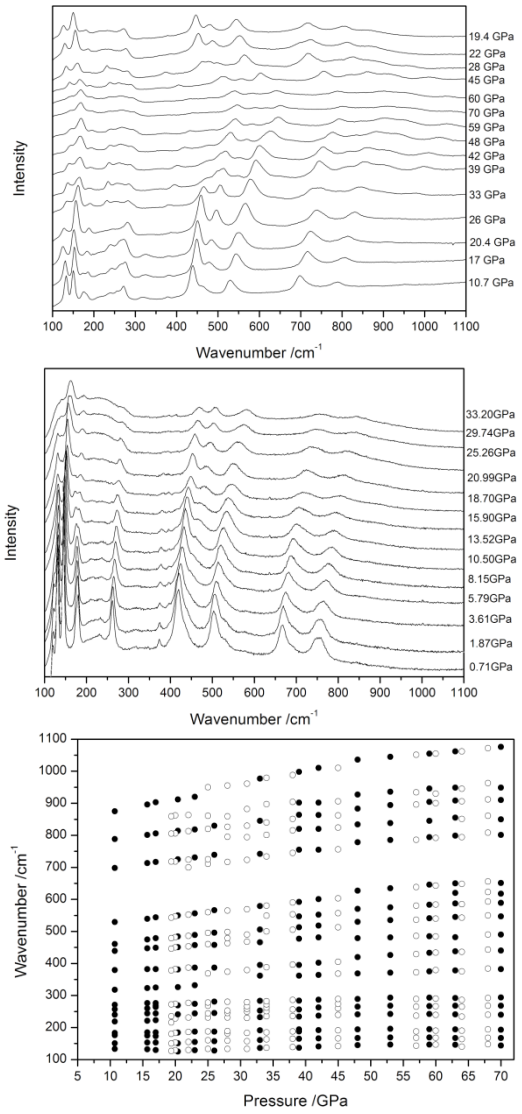

Figure 4. Top: Raman spectra of β-TaON during compression to 33 GPa. Centre: Raman spectra of TaON obtained during compression between 10-70 GPa followed by decompression to ambient pressure. Bottom: wavenumber values recorded for Raman peaks of TaON phases during compression to 70 GPa followed by decompression to ambient pressure.

Following those observations we collected additional Raman data to 70 GPa followed by decompression (Fig. 4). The dominant low wavenumber peaks (A_g, B_g at 131, 144 cm^{-1}) broaden and decrease in intensity especially above 25 GPa but both features can still be distinguished up to 70 GPa. The original intensity pattern begins to be recovered below 28 GPa on decompression. The sharp peaks at 181 and 260 cm^{-1} likewise decrease rapidly in intensity throughout the 10-33 GPa range, while the lower frequency feature appears to become doubled from 8-16 GPa (Fig 4). A

broad background feature emerges underlying the 130-300 cm^{-1} region above approximately 15-20 GPa. A new peak near 450 cm^{-1} appears to emerge from a high frequency shoulder of the 420 cm^{-1} band above 10-13 GPa and this remains as a separate feature during decompression to ambient. Following pressurization to 70 GPa the ambient pressure spectrum is essentially reproduced following recovery apart from this additional peak (Fig. 4). Thus although the Raman data do not show clear evidence for a polymorphic phase transition at a particular pressure, it is obvious that a major structural change occurs over a significant pressure range, and that this transformation is reversible but associated with significant hysteresis.

X-ray diffraction

Angle dispersive X-ray diffraction data were collected at DLS I15 (λ=0.4167 Å) during compression to 57.6 GPa at room temperature (Fig. 5). Pressure values were determined from the diffraction peaks of the LiF pressure-transmitting medium using a recently determined equation of state.[34] Throughout the experiment the LiF peaks remained sharp indicating the absence of any substantial pressure gradients throughout the sample chamber although intergrain contacts in the highly incompressible powdered material would certainly result in locally heterogeneous stress environments. This likely explains the broadening of sample peaks during initial compression.

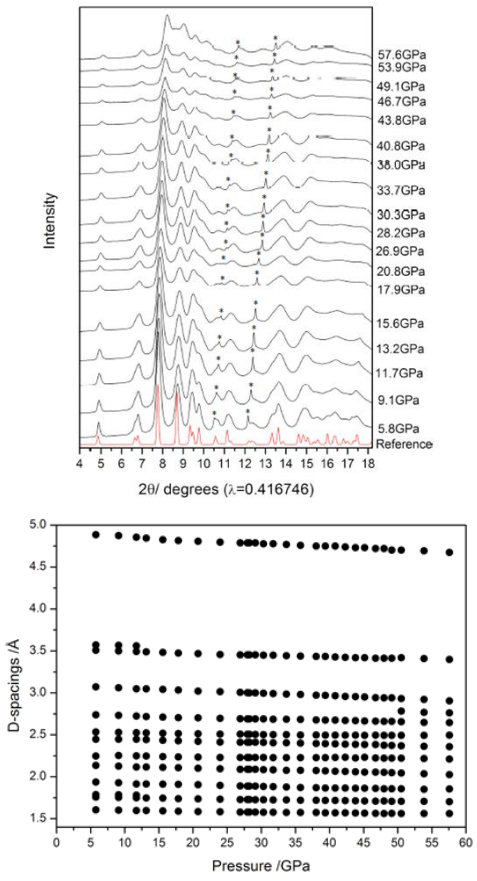

Figure 5. Top: Angle dispersive synchrotron XRD patterns of β-TaON compressed to 58 GPa using LiF as a pressure transmitting medium and standard. Sharp peaks marked with an asterisk (*) are due to LiF. The ambient pressure reference pattern is shown at bottom (red online).[10] Bottom: TaON d-spacings *vs* pressure.

The overall diffraction features of the β-TaON material appear to remain relatively unchanged until at least 40 GPa, and most elements of the starting pattern can still be discerned in the data obtained at 57.6 GPa. However some obvious changes are present especially above 40 GPa, with appearance of additional scattering between the main peaks at ~8 and 9° 2 θ that emerges as a new peak by above 44 GPa, and the evolution of a shoulder near 9° 2θ into a new double peak within the same pressure range. Plotting d_{hkl} values versus pressure did not reveal any obvious evidence for a structural phase transition, although slight inflections in the data sets appear to occur near 20-25 GPa and again above 50 GPa (Fig. 5). We continued our analysis by examining the *V(P)* relations obtained using Rietveld refinements of the data taking monoclinic baddeleyite structured β-TaON as a starting model.

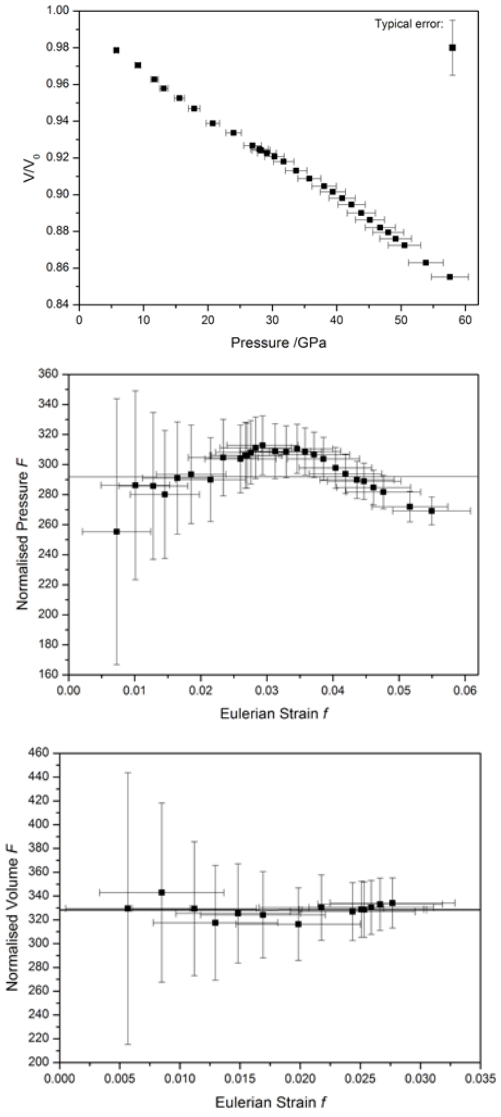

Figure 6. Pressure-volume relations in TaON at high pressure. Top: Plot of fractional unit cell volume of TaON refined using the ambient pressure $P2_1/c$ β-TaON structure as a model throughout the full pressure range. Centre: Plot of normalised pressure (*F*) vs Eulerian strain (*f*) during the compression of TaON from 6 to 58 GPa. Bottom: A plot of *F* vs *f* for β-TaON data up to the inflection in *V(P)* relation at P~24 GPa.

Rietveld refinements of the data proceeded smoothly up to approximately 25 GPa. However, the data became increasingly difficult to fit at higher pressures, mainly due to the emergence of additional scattering that could herald the onset of new reflections in the 8°-9° region, along with continued broadening and merging between other diffraction features throughout the pattern. We plotted *V(P)* relations obtained from these model fits, and these revealed the first evidence that a pressure-induced phase transition was present, signalled by a physically unreasonable[35] upward inflection in the 20-25 GPa range (Fig. 6).

To focus further on this observation we transformed the data into a dimensionless Eulerian stress-strain *(F-f)* diagram (Fig. 6). High pressure *V(P)* data for ceramic materials are typically fit using a Birch-Murnaghan equation of state (EoS) expanded to third order (BM3) [36,37]:

$$P(V) = 3K_o f(1+2f)^{5/2}\left(1+\frac{3}{2}(K_o'-4)f\right)$$

with the Eulerian strain parameter *f* given by

$$f = \frac{1}{2}\left[\left(\frac{V_o}{V}\right)^{2/3} - 1\right]$$

To simplify analysis K_o' is typically set to 4 and the *V(P)* curve analyzed using least squares methods to estimate K_o. However additional information can be derived by reducing the pressure to a dimensionless stress variable *via*:

$$F = P\left(3f(1+2f)^{5/2}\right)^{-1}$$

Plotting *F vs f* should result in a linear relation that returns values of K_o' and K_o related to the slope and intercept as $F \rightarrow 0$ for a single phase subjected to isotropic compression. However, if a phase transformation is present then this will appear as an unexpected change in slope in the *F(f)* plot (Fig. 6).

An obvious maximum is present in the *F-f* relation indicating a large change in mechanical properties that could be related to a polymorphic structural transformation. The change in slope is maximized between Eulerian strain values *f* ~0.026-0.037 corresponding to applied pressures in the 25-35 GPa range. However the onset pressure may occur at lower values. We can use the linearized *F-f* plot up to P ~ 20 GPa that corresponds to the first inflection in the *V(P)* data to estimate the compressibility properties of the low density baddeleyite structured polymorph (Fig. 6). That result returned K_0 = 328(4) GPa with K_0' = 4.3(15) with V_0 = 129.0266(4) Å^3, indicating that □-TaON is significantly (16%) less compressible than predicted theoretically.[14] However, the effect of the high pressure phase transformation on the *V(P)* relations along with non-hydrostatic compression conditions present within the sample could affect this value. Those points are discussed further below.

Because of peak broadening and the likely presence of multiple phases we could not obtain unique solutions for Rietveld fits to the diffraction data. However, we could identify the likely candidate for the high pressure TaON phase as the cotunnite structured compound predicted to become stable above 30 GPa [17,18] by comparing the X-ray diffraction pattern obtained at high pressure with different structural models (Fig. 7). Only the orthorhombic (*Pnma*) cotunnite phase shows a good match with the experimental pattern. The diffraction pattern of the cotunnite structure is very

similar to that of the starting baddeleyite □-TaON phase thus contributing to the difficulty in clearly identifying the phase transition from diffraction studies. However, the transition is not complete even at the highest pressure examined in the X-ray diffraction study. Two peaks near 5 and 7° and features in the 8-10° 2θ range remain from the starting baddeleyite structured polymorph. That result indicates that the transformation kinetics are extremely slow at room temperature, but cannot be used to infer information about the magnitude of the thermodynamic change (-PΔV) for the transition. Similarly slow kinetics have been reported previously for ZrO_2.[16] In addition, part of the intensity of the feature near 5° 2θ could also be due to the presence of material with the tetragonal bismoclite (BiOCl) structure that is predicted theoretically to exist above 38 GPa [17].

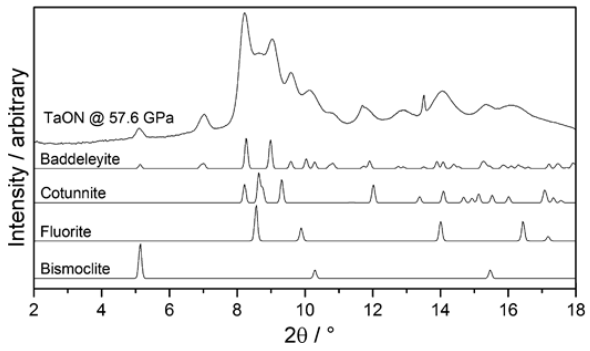

Figure 7. A comparison of the experimentally observed XRD pattern of TaON at 57.6 GPa, with the calculated patterns of β-TaON (baddeleyite), and cotunnite-, fluorite- and bismoclite-type structures that have been predicted to exist theoretically to exist at high pressure (plotted with pressure-appropriate lattice parameters).[12,17,18]

The Raman spectrum of the sample at 70 GPa is also consistent with assignment to a cottunite structured phase (Fig. 8). As for the baddeleyite phase, symmetry analysis indicates that 18 bands are expected:

$$\Gamma_{Raman} = 6A_g + 3B_{1g} + 6B_{2g} + 3B_{3g}.$$

The large number of bands observed (at 144, 167, 193, 240, 268, 294, 382, 440, 490, 547, 589, 618, 651, 801, 850, 910, 949 and 1076 cm^{-1}) is most consistent with this assignment, although the peaks are expected to occur in similar positions to those of the starting β-TaON phase but with a different relative intensity pattern. Tetragonal or cubic phases would exhibit many fewer peaks, although these features might also be present within the pattern. On decompression the β-TaON spectrum is recovered with most reversible changes occurring in the 28-25 GPa range (Fig. 4). As noted earlier, one additional band at 450 cm^{-1} remains in the fully decompressed spectrum indicating that the reverse transition is equally sluggish, and that some of the high pressure phase persists at ambient conditions.

We could gain an initial estimate of the bulk modulus for the cotunnite-structured phase by extrapolating the linear portion of the *F-f* plot above the inflection point ($f > 0.035$) back to the intercept with the *F* axis. This yields an estimated K_o ~370 GPa (Fig. 7), that lies remarkably (and most likely fortuitously) close to the value predicted by DFT calculations [18]. From the X-ray and Raman results discussed above it is certain that although the phase transition pressure appears to be centered around 30-35 GPa corresponding to the theoretical prediction, the transformation kinetics are slow and substantial fractions of both phase persist to 58 GPa or above. In addition other

polymorphs such as the bismoclite-structured TaON predicted by theory to exist above 38 GPa might also be present in the sample. In addition to these effects the compression environment within the powdered sample is certainly non-hydrostatic due to intergrain contacts and geometric changes due to the phase transition. All these effects will cause the determined elastic parameters to vary but it appears certain that the cotunnite-structured phase has very low compressibility, that is likely to be even smaller than that observed for ZrO_2 [16].

High pressure XAS and EXAFS studies

We carried out a detailed study of local structural changes in TaON during compression to 45 GPa followed by decompression by EXAFS analysis and modelling. The Ta L_3 absorption edge and near edge-structure data measured during the compression and decompression runs are shown in Fig. 8. A small glitch from the diamonds appears at the top of the white line but its constant position throughout the runs allowed a reasonable value for E_0 to be obtained from the first derivative of data in this spectral region.

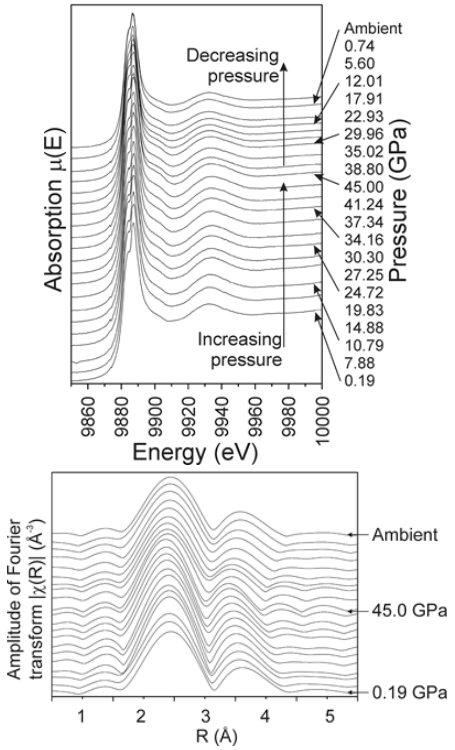

Figure 8. XAS and EXAFS data of TaON during compression to 45 GPa. Top: Ta L_3 absorption edge data. Bottom: Fourier transformed EXAFS data.

The shape of this region of the spectrum is weakly affected by pressure: a small bump appears after the white line, at ~ 9900 eV, while the first EXAFS oscillation at 9930 eV in slightly enhanced. Both these features are reversible upon decompression. Fig. 8 illustrates the evolution, again upon compression and decompression, of the amplitude of the Fourier Transform of the EXAFS oscillations in the k-range (2.75-7.05 $Å^{-1}$). This figure provides a first qualitative picture of the evolution with pressure of the first two shells of neighbours of Ta: a first shell composed of O/N atoms at ~ 2 Å, and a second shell composed of Ta atoms at ~3.2 Å (the abscissa in this plot is not corrected for phase shifts). Whereas a strong (reversible) compression is evident for the Ta-Ta shell, the Ta-O/N shell

appears much more rigid upon compression. However, this first shell is seen to expand upon decompression (Fig. 9).

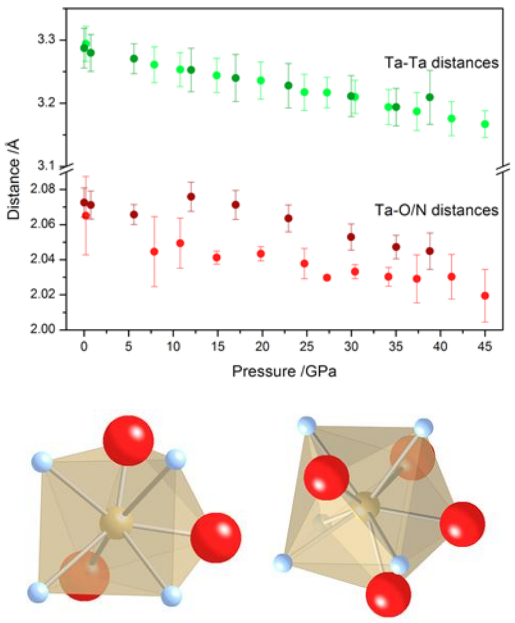

Figure 9. Top: best fit Ta-O/N and Ta-Ta distances during compression (bright red and green respectively) and decompression (dark red and green respectively). Bottom: sketch of Ta-(O,N) coordination environments in baddeleyite (left) and cotunnite (right) structures.

In order to obtain more quantitative information, the high-pressure TaON data were analyzed by fitting to structural models generated *via* FEFF[30,31] using ARTEMIS[28,29]. The initial structure model was developed by considering first and second shells based on the room pressure data for the □-TaON polymorph. Refined fits included Ta-(O,N) and Ta...Ta scattering paths: attempts to distinguish independent O and N scattering path contributions yielded inconclusive results, therefore only Ta-N paths were included. The ambient pressure data was fitted in the k-range (2.8-13.4 $Å^{-1}$). The local structure around Ta, in the R-range (1.0-3.3 Å) could be described using a first shell containing one Ta-O/N path with degeneracy 3 and a second Ta-O/N path with degeneracy 4. The second shell contains seven Ta atoms at three distinct distances around an average value of 3.27 Å. This was modelled by a single Ta-Ta path with degeneracy 7 A total of 8 fitting parameters were used for this fit: one distance and one mean square relative displacement for each path, and the two non-structural parameters E_0 and S_0^2 . Best fit structural parameters are listed in Table 3.

Table 3. Best fit parameters for the ambient pressure structure.

Path	**Type**	**N**	**R / Å**	**σ^2**
Path 1	Ta—O/N	4	2.05±0.01	0.003±0.003
Path 2	Ta—O/N	3	2.17±0.02	0.003±0.003
Path 3	Ta—Ta	7	3.30±0.01	0.006±0.001

Due to the significantly smaller k range available for the high pressure data (2.75-7.05 $Å^{-1}$) the fitting was simplified to a single Ta-O/N path and one Ta-Ta path, both with degeneracy 7. Only 4 fitting parameters were used for the high pressure data: one distance and one mean square relative displacement for each path. Values of the non-structural parameters E_0 and S_0^2 were fixed to the best fit values found for the ambient P data: E_0= 10.0 ± 0.5 eV and S_0^2 = 0.90 ± 0.06.

The best fit values of the average Ta-O/N and Ta-Ta distances are shown in Figure 9. Both first and second shell distances shift to smaller values as expected at high pressure. The Ta-Ta values decrease by approximately 3.2% between ambient and 45 GPa consistent with the change in unit cell volume (Fig. 6). These values appear to be completely reversible upon decompression. The decrease in Ta-(O,N) distances is smaller (<2%) and some hysteresis appears to be present during decompression, consistent with the sluggish phase transition observed by XRD, with slightly longer bond lengths achieved in the material following high P treatment. That could indicate the partial retention of the high density cotunnite structure that has its metal-oxygen polyhedra in higher coordination environments with Ta atoms surrounded by 9 (4O + 5N) *vs* 7 (3O + 4N) anions (Fig. 9).

Conclusions

Our results support the existence of a pressure induced phase transition occurring between □-TaON and a cotunnite structured phase in the 25-35 GPa range as predicted theoretically. The structural transformation is kinetically impeded at ambient temperature and exhibits substantial hysteresis during both pressurization and decompression cycles. Similar behavior was observed previously for isoelectronic ZrO_2. The low pressure baddeleyite structured phase has K_o = 328(4) GPa that is higher than the value predicted by DFT calculations. However the experimental data analysis may be hampered by the presence of the phase transformation as well as non-hydrostatic local compression conditions within the polycrystalline sample. The high pressure cotunnite structured phase is estimated to have a very K_o value of at least 370 GPa in agreement with theoretical predictions.

Acknowledgements

This work was supported by an EPSRC Senior Research Fellowship award to PFM. Additional ESRF funding helped support a long term visit by KEW (now Seeow) to ID24. The authors thank ESRF and Diamond Light Source for access to beamlines.

Notes and references

[1] M. Jansen and H. P. Letschert, *Nature*, 2000, **404**, 980-982.

[2] E. Guenther and M. Jansen, *Mater. Res. Bull.*, 2001, **36**, 1399-1405.

[3] Y. Moriya, T. Takata and K. Domen, *Coord. Chem. Rev.*, 2013, **257**, 1957-1969.

[4] K. Domen, M. Hara, J. N. Kondo, T. Takata, A. Kudo, H. Kobayashi and Y. Inoue, *Korean J. Chem. Eng.*, 2001, **18**, 862-866.

[5] K. Maeda and K. Domen, *J. Phys. Chem. C*, 2007, **111**, 7851-7861.

[6] K. Maeda, H. Terashima, K. Kase and K. Domen, *Appl. Catal. A: General*, 2009, **357**, 206-212.

[7] G. Brauer and J. R. Weidlein, *Angew. Chem. Intl. Ed. Engl.*, 1965, **4**, 875.

[8] D. Armytage and B. E. F. Fender, *Acta Crystall. B*, 1974, **30**, 809-812.

[9] M. Weishaupt and J. Strähle, *Z. Anorg. Allg. Chem.*, 1977, **429**, 261-269.

[10] M. Yashima, Y. Lee and K. Domen, *Chem. Mater.*, 2007, **19**, 588-593.

[11] Q. S. Gao, C. Giordano and M. Antonietti, *Small*, 2011, **7**, 3334-3340.

[12] H. Schilling, A. Stork, E. Irran, H. Wolff, T. Bredow, R. Dronskowski and M. Lerch, *Angew. Chem. Intl. Ed.*, 2007, **46**, 2931-2934.

[13] M. W. Lumey and R. Dronskrowski, *Z. Anorg. Allg. Chem.*, 2003, **629**, 2173.

[14] C. M. Fang, E. Orhan, G. A. de Wijs, H. T. Hintzen, R. A. de Groot, M. R., J.-Y. Saillard and G. de With, *J. Mater. Chem.*, 2001, **11**, 1248-1252.

[15] H. Wolff, T. Bredow, M. Lerch, H. Schilling, E. Irran, A. Stork and R. Dronskowski, *J. Phys. Chem. A*, 2007, **111**, 2745-2749.

[16] J. Haines, J. M. Léger and A. Atouf, *J. Amer. Ceram. Soc.*, 1995, **78**, 445-448.

[17] M.-W. Lumey and R. Dronskowski, *Z. Anorg. Allg. Chem.*, 2005, **631**, 887-893.

[18] J. E. Lowther, *Phys. Rev. B*, 2006, **72**, 172105.

[19] W. R. Matizamhuka, I. Sigalas and M. Herrmann, *Ceram. Intl.*, 2008, **34**, 1481-1486.

[20] F. Tessier and R. Marchand, *J. Solid State. Chem.*, 2003, **171**, 143-151.

[21] S. J. Henderson and A. L. Hector, *J. Solid State Chem.*, 2006, **179**, 3518-3524.

[22] A. C. Larson and R. B. Von Dreele, "General Structure Analysis System (GSAS)", Los Alamos National Laboratory report LAUR 86-748 (2004); B. H. Toby, *J. Appl. Cryst.*, 2001, **34**, 210-213.

[23] E. Soignard and P. F. McMillan, *Chem. Mater.*, 2004, **16**, 3533-3542.

[24] A. P. Hammersley, S. O. Svensson, M. Hanfland, A. N. Fitchand D. Häusermann, *High Press. Res.*, 1996, **14**, 235-248.

[25] A. J. Dent, G. Cibin, S. Ramos, A. D. Smith, S. M. Scott, L. Varandas, M. R. Pearson, N. A. Krumpa, C. P. Jones and P. E. Robbins, *J. Phys.: Conf. Ser.*, 2009, **190**, 012039.

[26] S. Pascarelli, O. Mathon, M. Munoz, T. Mairs and J. Susini, *J. Synchr. Rad.*, 2006, **13**, 351.

[27] Ravel, B., 2003. EXAFS analysis software using IFEFFIT. *http://feff.phys.washington.edu/~ravel/software/exafs/*

[28] M. Newville, *J. Synchrotron Rad.*, 2001, 8, 322-324

[29] B. Ravel and M. Newville, *J. Synchrotron Rad.*, 2005, 12, 537-541.

[30] S. I. Zabinsky, J. J. Rehr, A. Ankudinov, R. C. Albers and M. J. Eller, *Phys. Rev. B*, 1995, **52**, 2995-3009.

[31] J.J. Rehr & R.C. Albers, *Rev. Mod. Phys.* (2000) **72**, 621-654

[32] P. Li, W. Fan, Y. Li, H. Sun, X. Cheng, X. Zhao and M. Jiang, *Inorg. Chem.*, 2010, **49**, 6917-6924.

[33] R. Nakamura, T. Tanaka and Y. Nakato, *J. Phys. Chem. B*, 2005,**109**, 8920-8927.

[34] J. Liu, L. Dubrovinsky, T. Boffa Ballaran and W. Crichton, *High Press. Res.*, 2007, **27**, 483-489.

[35] D. C. Wallace, *Thermodynamics of Crystals*, John Wiley & Sons, Inc., New York, 1972.

[36] F. Birch, *Phys. Rev.*, 1947, **71**, 809-824

[37] F. D. Murnaghan, *Proc. Natl. Acad. Sci. USA*, 1944, **30**, 244-247.